Available online at www.sciencedirect.com
ScienceDirect
Journal of Molecular Catalysis A: Chemical 271 (2007) 200–208
JOURNAL OF MOLECULAR CATALYSIS A: CHEMICAL
www.elsevier.com/locate/molcata

Large-pore cubic Ia-3d mesoporous silicas: Synthesis, modification and catalytic applications

Jiahui Huang [a], Ge Tian [b], Hongsu Wang [a], Ling Xu [a], Qiubin Kan [a,*]

[a] *Department of Chemistry, Jilin University, Changchun 130023, China*
[b] *Department of Chemistry & State Key Laboratory of Inorganic Synthesis and Preparative Chemistry, Jilin University, Changchun 130023, China*

Received 24 July 2006; received in revised form 12 February 2007; accepted 19 February 2007
Available online 22 February 2007

Abstract

Large-pore cubic Ia-3d mesoporous silicas were synthesized by co-condensation of tetraethoxysilane (TEOS) and a small amount of phenyltriethoxysilane (PTES) under acidic conditions using triblock copolymer P123 ($EO_{20}PO_{70}EO_{20}$) as the template. In the synthesis procedure, the amount of PTES added in the range of 3.0–10% was very vital for the formation of the ordered Ia-3d structure. In addition, the prehydrolysis of PTES prior to TEOS in the template solution was also important for the preparation of ordered Ia-3d materials. If TEOS was prehydrolyzed, ordered 2d-hexagonal materials were obtained. After mild calcination at 250 °C to selectively remove the template, Ia-3d and 2d-hexagonal materials with 10% PTES were selected to be sulfonated to introduce sulfonic acid sites into the channels. Both Ia-3d and 2d-hexagonal mesoporous sulfonic acid catalysts can effectively catalyze the liquid phase condensation reaction of phenol with acetone to Bisphenol A. The catalytic activity of the Ia-3d catalyst was slightly higher than that of the 2d-hexagonal one. Additionally, after calcination at 550 °C to remove the template and phenyl groups, Ia-3d mesoporous materials with different pore sizes (3.8–6.8 nm) were further functionalized with amino groups by postsynthesis grafting. It was found that in the synthesis of flavanone the catalytic performance of amino-functionalized Ia-3d mesoporous base catalysts increased with the increase in their pore sizes.

Keywords: Mesoporous silicas; Cubic Ia-3d; Bisphenol A; Flavanone

1. Introduction

Since the discovery of the ordered mesoporous MCM-41S family [1], a great variety of mesoporous materials have been obtained. Due to their high specific surface areas, uniform mesoporous channels and excellent mechanical stability, the potential applications of these materials in adsorption and catalysis have attracted much attention [2–4]. The heteroatom-substituted mesoporous materials have been widely studied for catalyzing many reactions. To develop new catalytic applications of mesoporous materials, much attention has been paid to the immobilization of various organic groups, which contain active sites or can be further modified to introduce active components, to the pore surface of mesoporous materials by postsynthesis grafting or co-condensation. Until now, various organic groups such as phenyl, octyl, mercapto, amino, vinyl, methacrylate and cyclodextrin were anchored to the pore surface of mesoporous materials MCM-41, MCM-48, HMS, MSU, etc. However, the relatively small pore sizes (<4 nm) of these organic–inorganic mesoporous materials would probably limit their potential applications in the catalysis field, especially in the reactions of bulky molecules. Fortunately, the synthesis of SBA-15 [5,6] and its hybrid derivates [7–11] resulted in the formation of large pores (>5 nm), which makes the efficient diffusion and reactions of bulky molecules possible.

Compared with the two-dimensional channels of 2d-hexagonal SBA-15 materials, the independent and intricately interwoven three-dimensional channels of large-pore (>5 nm) Ia-3d materials are more beneficial to the diffusion and transport of reactants and products in catalytic reactions. Up to now, there are some reports about the synthesis of large-pore (>5 nm) Ia-3d materials [12–17]. However, these studies have only focused on the preparation of Ia-3d materials, but not on their applications such as in catalysis.

* Corresponding author. Tel.: +86 431 8499140; fax: +86 431 8949334.
E-mail address: qkan@mail.jlu.edu.cn (Q. Kan).

1381-1169/$ – see front matter © 2007 Published by Elsevier B.V.
doi:10.1016/j.molcata.2007.02.024

We have reported in a short communication that large-pore cubic Ia-3d mesoporous materials can be prepared by virtue of the addition of 3.0–8.0% PTES in the synthesis system [18]. In this study, by lowering the ageing temperature from 50 °C to 35 °C, large-pore cubic Ia-3d mesoporous materials have been obtained in the range of 3.0–10% PTES. In addition, here we have also found that the prehydrolysis of PTES prior to TEOS in the template solution was very important for the preparation of cubic Ia-3d materials. If TEOS was prehydrolyzed, phenyl-functionalized 2d-hexagonal mesoporous materials were obtained.

By the sulfonation of phenyl groups, sulfonic acid sites were introduced into the channels of mildly calcined (250 °C) Ia-3d materials. Additionally, by postsynthesis grafting, amino groups were introduced into the channels of calcined (550 °C) Ia-3d materials. These phenyl-sulfonic acid functionalized Ia-3d mesoporous acid catalysts and amino-functionalized Ia-3d mesoporous base catalysts were found to be very efficient in the synthesis of Bisphenol A and flavanone, respectively.

2. Experimental

2.1. Synthesis of large pore phenyl-functionalized cubic Ia-3d mesoporous silicas

A typical synthesis procedure of large-pore cubic Ia-3d mesoporous silicas was as follows: 1.5 g of P123 ($EO_{20}PO_{70}EO_{20}$, MW = 5800, Aldrich) was dissolved in 40 mL of 0.75 M HCl at 35 °C, and then 15.2*X* mmol of phenyltriethoxysilane (PTES, Aldrich) was added under vigorous stirring. After vigorous stirring for 15 min, 15.2 $(1 - X)$ mmol of tetraethoxysilane (TEOS) was added and the mixture was further stirred at 35 °C for 20 h. The final gel composition (mol) was 0.017 P123:$(1 - X)$ TEOS:*X* PTES:2.0 HCl:147 H_2O ($X = 0.03$–0.10). The reactant mixture was transferred into a Teflon-lined stainless steel autoclave and then aged at the required temperature for 24 h. After cooling down to the room temperature, the product was filtered, washed with distilled water repeatedly and then dried at 60 °C in air overnight. As-synthesized materials were denoted by $I_x(y)_a$, where *x* and *y*, respectively, represent the ageing temperature and the molar fraction of PTES in silicon sources.

2.2. Preparation of phenyl-sulfonic acid functionalized cubic Ia-3d mesoporous acid catalysts

As-synthesized materials were calcined at 250 °C in air for 6 h to selectively remove the template. One gram of the mildly calcined Ia-3d material was dried under vacuum at 120 °C overnight and then sulfonated with 25% fuming sulfuric acid in the presence of CH_2Cl_2 at room temperature for 5 h (25 mL of CH_2Cl_2 and 3 mL of 25% fuming sulfuric acid) [19]. After the reaction the sulfonated material was filtered, and washed with CH_2Cl_2 and then distilled water until the filtrate was neutral. The solid thus obtained was denoted by $I_x(y)$-SO_3H.

2.3. Preparation of amino-functionalized cubic Ia-3d mesoporous base catalysts

As-synthesized materials were calcined at 550 °C in air for 6 h to remove the template and phenyl groups. One gram of the calcined Ia-3d material was dried under vacuum at 120 °C overnight, and then added to 20 mL of dry toluene in a 50 mL flask. Then 0.4 mL of 3-aminopropyltriethoxysilane (APTES) was added and the mixture was stirred. After 24 h, the solid was filtered, washed with toluene and ethanol, and then dried in air. The obtained solid was denoted by $I_x(y)$-APS.

2.4. Characterization

Powder X-ray diffraction (XRD) patterns were obtained on a Siemens D5005 diffractometer using Cu Kα radiation. Transmission electron microscopy experiments were performed on a Hitachi H-8100 electron microscope with an acceleration voltage of 200 kV. N_2 adsorption–desorption isotherms were recorded at 77 K with a Micromeritics ASAP 2010. Before the measurements, the samples were outgassed at 120 °C for 10 h. The BET surface areas were obtained from the adsorption branches in the relative pressure range of 0.05–0.20. The pore size distributions were calculated from the adsorption branches by the Barret–Joyner–Halenda (BJH) method. The pore volume was taken at the relative pressure of 0.97. The ^{29}Si MAS NMR and ^{13}C CP/MAS NMR spectra were recorded on a Bruker DRX-400 system equipped with a magic-angle spin probe in a 4-mm ZrO_2 rotor. The ^{29}Si MAS NMR spectra were recorded at 79.4 MHz, with a pulse delay of 2.0 s, acquisition time of 16.9 ms, and spinning rate of 4 kHz. The ^{13}C CP/MAS NMR spectra were recorded at 100.5 MHz, with a pulse delay of 3.0 s, acquisition time of 17.1 ms, and spinning rate of 4 kHz. Tetramethylsilane was used as a reference. TG analysis was measured on a DTG-60 apparatus (Shimadzu) at a heating rate of 10 °C/min in air. N, C and S elemental analyses were performed on a Heraeus CHNS elemental analyzer. The acid amount of the sulfonated material was determined by base titration. Typically, 0.05 g of the solid was immersed in 30 g of sodium chloride aqueous solution (10 wt%) for 24 h. The resulting suspension was filtered and the filtrate was titrated by dropwise addition of 0.05 M NaOH (aq).

2.5. Catalytic reactions

The syntheses of Bisphenol A and flavanone were carried out in a sealed glass vessel. Before the reaction, both mesoporous acid and base catalysts were dried under vacuum at 120 °C overnight. For the synthesis of Bisphenol A, 60 mmol of phenol and 10 mmol of acetone were added to a flask containing 0.10 g of the dried mesoporous phenyl-sulfonic acid catalyst. The reaction mixture was stirred at 85 °C for 24 h, and then a small amount of acetonitrile was added and then the mixture was filtered. The products were analyzed on a gas chromatograph (GC-8A, Shimadzu) equipped with an HP-5 capillary column, and confirmed by standard compounds. For the synthesis of flavanone, 10 mmol of benzaldehyde and 10 mmol of

2′-hydroxyacetonphenone were added to a flask with 0.20 g of the dried amino-functionalized mesoporous base catalyst. The reaction mixtures were stirred at 140 °C for 15 h, and then 5 mL of dimethyl sulfoxide (DMSO) was added and then the mixture was filtered. The filtrate was analyzed on a gas chromatograph (GC-8A, Shimadzu) equipped with an HP-5 capillary column, and confirmed by GC–MS.

3. Results and discussion

3.1. Large pore phenyl-functionalized cubic Ia-3d mesoporous silicas

Based on the powder XRD diffraction analysis (Fig. 1), it is found that in the synthesis procedure the amount of PTES added to the template solution plays a very crucial role in obtaining the ordered Ia-3d materials. If no PTES is added or the amount of PTES added is less than 3.0%, only the ordered 2d-hexagonal SBA-15 or SBA-15-like material is obtained. When the amount of PTES is elevated to 3.0%, the characteristic diffraction peaks (1 1 0) and (2 0 0) of the 2d-hexagonal material disappear, and a well-defined shoulder peak and a broad diffraction peak in the range of $2\theta = 1.3$–2.0° are observed, suggesting the transition from the 2d-hexagonal SBA-15-like symmetry to the Ia-3d structure. With further increasing amount of PTES to 5.0%, the ordered material with Ia-3d symmetry can be easily obtained, which exhibits an intense peak indexed as (2 1 1) and a shoulder peak indexed as (2 2 0) in the XRD pattern [12–15]. The other 4-weak peaks in the range of $2\theta = 1.3$–2.0° can also be observed, which are indexed as (3 2 1), (4 0 0), (4 2 0) and (3 3 2) reflections, respectively. This well-defined Ia-3d structure can be further confirmed by TEM images. The electron micrographs in Fig. 2 are taken along [1 1 1], [1 1 0], [1 0 0] directions, respectively. These images show that the ordered Ia-3d structure is throughout the sample. At 10% PTES, the ordered Ia-3d material can still be obtained, but its cell parameter obviously shrinks in comparison to that $I_{100}(0.05)$ (Table 1). At higher amounts of PTES, e.g. 15%, the amorphous material is obtained. The effect of PTES/(PTES + TEOS) ratio (3.0–10%) on the phase behavior of the synthesized system may be explained as follows: since phenyl groups are hydrophobic, they will be preferentially bound to the hydrophobic PPO blocks than to the hydrophilic PEO blocks, enlarging the hydrophobic volume and increasing the hydrophobic/hydrophilic ratio. Finally these changes will lead to the phase transition from high-curvature 2d-hexagonal to low-curvature Ia-3d symmetry. This phenomenon has also been observed when 3-mercaptopropyltrimethoxysilane (MPTS) [12], triethoxyvinylsilane (TEVS) [14], butanol [15], or anionic sodium dodecyl sulfate (SDS) [17] was used as additives for the synthesis of Ia-3d materials. If the PTES/(PTES + TEOS) ratio is reduced to 1.0%, the amount of hydrophobic phenyl groups is not high enough to significantly enlarge the hydrophobic/hydrophilic ratio, and thus the ordered Ia-3d structure cannot be formed. If this value is increased to 15% or more, the self-assembly between copolymer template and silicon sources will be disturbed, and only the amorphous material is formed.

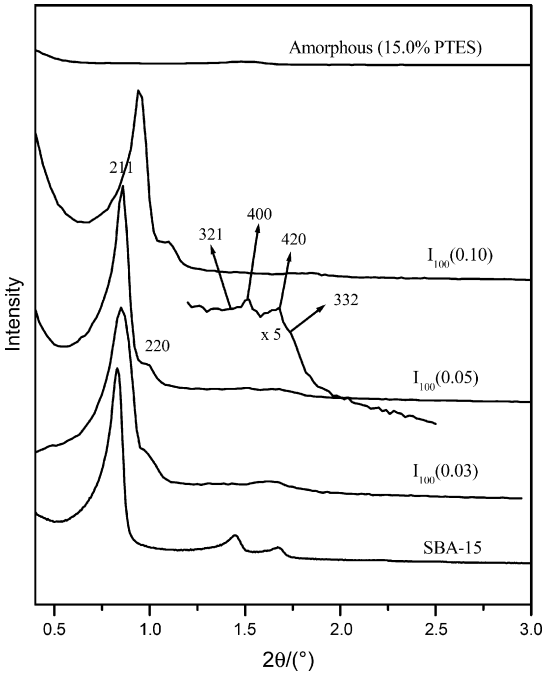

Fig. 1. Powder XRD patterns of mildly calcined (250 °C) purely siliceous SBA-15, $I_{100}(0.03)$, $I_{100}(0.05)$, $I_{100}(0.10)$ and amorphous material contanining 15% PTES.

It is well known that the elevation of ageing temperature will lead to the increase in the hydrophobicity of EO block moiety in triblcok copolymer and then the increase in the hydrophobic volume of surfactant micells, finally resulting in the enlargement of pore dimension of mesoporous silica [6]. Here, we investigated the effect of ageing temperature on the pore structures of phenyl-functionalized Ia-3d mesoporous materials with 5.0% PTES. The powder XRD patterns of the materials aged at different temperature are shown in Fig. 3. Ia-3d materials are obtained at all the ageing temperature, but the elevated temperature makes diffraction peaks more intense and much clearer. For the material aged at 35 °C, only (2 1 1) and (2 2 0) diffraction peaks can be observed, and the broad peak in the range of 1.3–2.0° (2θ) is absent. However, at the ageing temperature of 80 °C, 100 °C or 130 °C, the characteristic diffraction peaks of Ia-3d materials can be easily observed. For these materials, the structural improvement with the increase in ageing temperature can also be confirmed by the nitrogen adsorption–desorption isotherms

Table 1
Physicochemical properties of mildly calcined (250 °C) phenyl-functionalized Ia-3d mesoporous materials

Sample	Phase	a_0[a] (nm)	S_{BET} ($m^2\,g^{-1}$)	Pore size (nm)	V_t ($cm^3\,g^{-1}$)
SBA-15	2d-hexagonal	12.3	925	8.8	1.39
$I_{100}(0.03)$	Ia-3d	25.5	1152	7.5	1.30
$I_{35}(0.05)$	Ia-3d	22.1	805	4.2	0.48
$I_{80}(0.05)$	Ia-3d	24.7	1072	6.1	0.84
$I_{100}(0.05)$	Ia-3d	25.2	1091	7.2	1.21
$I_{130}(0.05)$	Ia-3d	25.5	862	8.9	1.33
$I_{100}(0.10)$	Ia-3d	23.6	1022	5.3	1.03

[a] a_0: cell parameter.

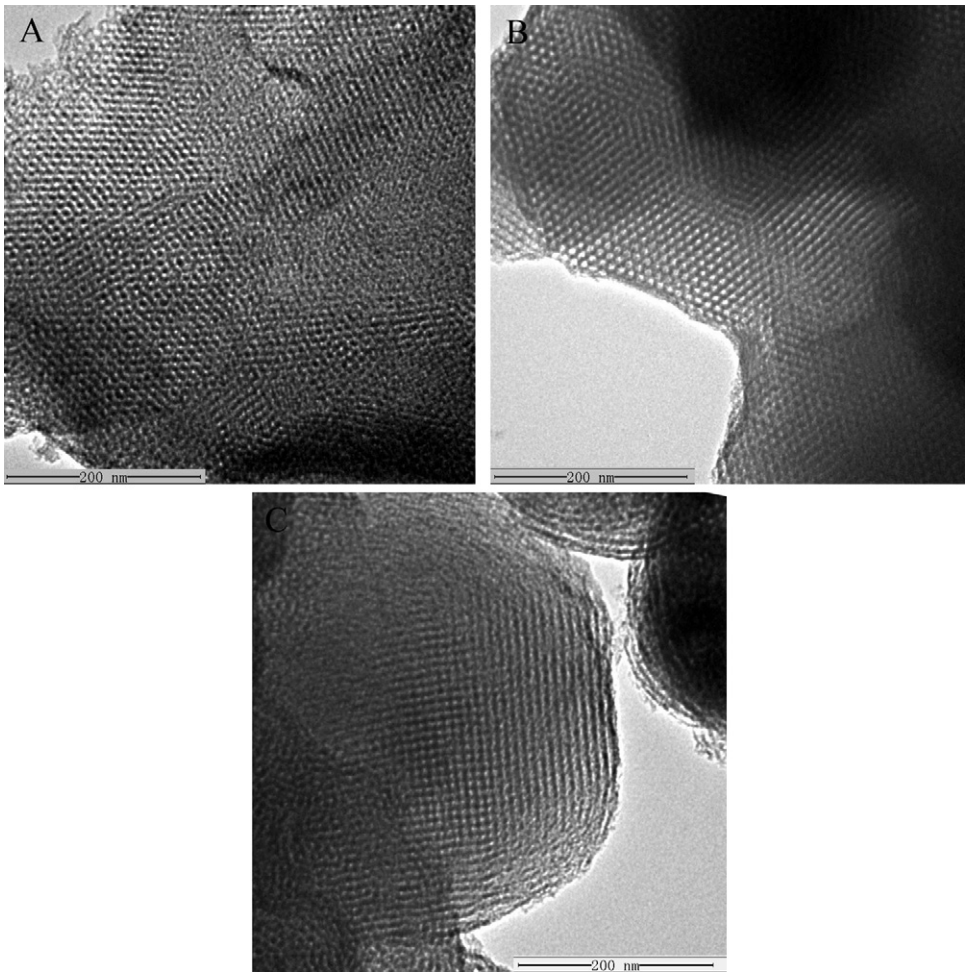

Fig. 2. TEM images of mildly calcined (250 °C) $I_{100}(0.05)$ along different directions: (A) [1 1 1], (B) [1 1 0] and (C) [1 0 0].

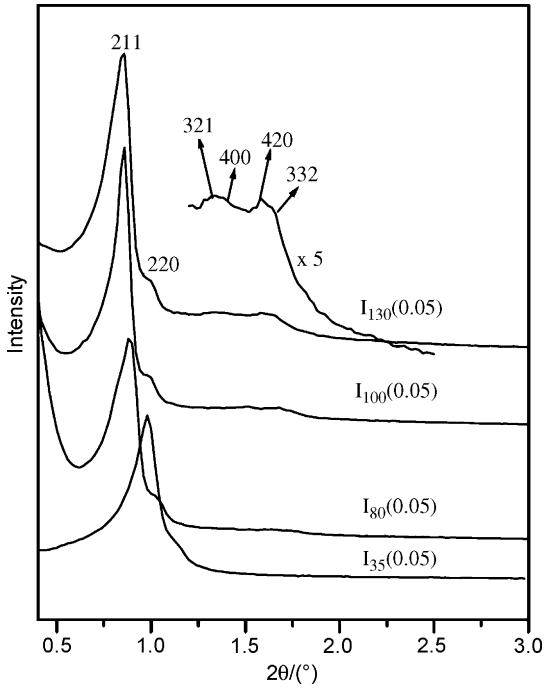

Fig. 3. Powder XRD patterns of mildly calcined (250 °C) $I_{35}(0.05)$, $I_{80}(0.05)$, $I_{100}(0.05)$ and $I_{130}(0.05)$.

and the pore size distributions (Fig. 4). These isotherms display typical IV isotherms with a sharp inflection due to the capillary condensation in the uniform mesopore channels and with a H1 type hysteresis loop which implies that these samples have bicontinuous mesopore channels without necks (Fig. 4A). With increasing ageing temperature, the inflection is shifted to the higher relative pressure, and the capillary condensation also becomes much steeper, indicating the enlargement of pore dimension and the narrowing of pore size distribution. The pore size distributions of these materials support this analysis (Fig. 4B). When the ageing temperature is elevated from 35 °C to 130 °C, the pore size is doubled from 4.2 nm to 8.9 nm, and the pore size distribution becomes more narrow. Meanwhile, the pore volume is also steeply increased from 0.48 $cm^3\ g^{-1}$ to 1.33 $cm^3\ g^{-1}$ (Table 1).

In the synthesis procedure of Ia-3d materials, besides the amount of PTES added, the prehydrolysis of PTES prior to TEOS in the surfactant solution is also important. For the material with 5.0% PTES, if PTES is added 15 min prior to TEOS into the template solution, the ordered Ia-3d material is obtained (Fig. 5a). If TEOS and PTES are mixed in advance and then added to the template solution, a mixture of 2d-hexagonal and Ia-3d structures is obtained (Fig. 5b). When TEOS is prehydrolyzed for 15 min or more, the well-defined 2d-hexagonal SBA-15-like

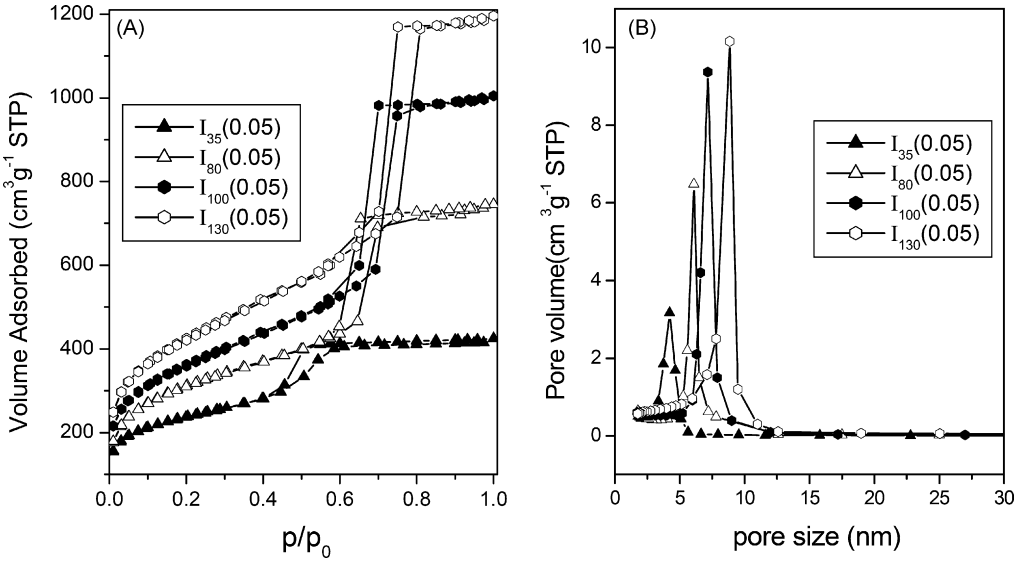

Fig. 4. N_2 adsorption–desorption isotherms (A) and pore size distributions (B) of mildly calcined (250 °C) $I_{35}(0.05)$, $I_{80}(0.05)$, $I_{100}(0.05)$ and $I_{130}(0.05)$.

materials are formed (Fig. 5c and d). The pronounced effect of prehydrolysis period of PTES or TEOS on the special structure of synthesized material might be explained as follows: during the synthesis procedure, if PTES is added 15 min prior to TEOS into the surfactant solution, the hydrophobic phenyl groups will be preferentially bound to the hydrophobic PO blocks, finally causing the phase transition from high-curvature 2d-hexagonal to low-curvature Ia-3d phase (Fig. 5a). If PTES and TEOS are mixed in advance and then co-condensed in the surfactant solution, the phenyl groups in PTES cannot be entirely bound to the hydrophobic PO blocks before the formation of mesoporous material. Therefore, only those surfactants well bound by phenyl groups can direct the formation of the Ia-3d structure, and the left will result in the formation of the 2d-hexagonal structure (Fig. 5b). If TEOS is prehydrolyzed 15 min or more prior to PTES in the template solution, the surfactant micelles will be covered with some polymeric silicas, making it very difficult for the hydrophobic phenyl groups to be bound to hydrophobic PO blocks, resulting in the synthesis of 2d-hexagonal material (Fig. 5c and d). A similar phenomenon is also observed for the synthesis of the material with 10% PTES (not shown).

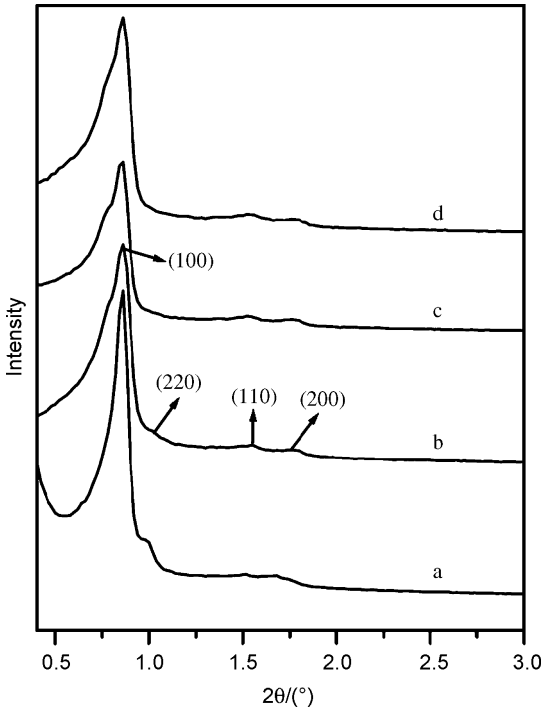

Fig. 5. Powder XRD patterns of mildly calcined (250 °C) Ia-3d $I_{100}(0.05)$ (a), 2d-hexagonal materials with TEOS prehydrolyzed for 0 min (b), 15 min (c) and 30 min (d) (a small amount of cubic structure is present in the material (b)).

Fig. 6 displays the ^{29}Si MAS NMR and ^{13}C CP/MAS NMR spectra of phenyl-functionalized Ia-3d mesoporous materials. As shown in Fig. 6A, the resonance peaks at −109.0 ppm and −100.3 ppm are assigned to Q^4 [$Si(OSi)_4$] and Q^3 [$Si(OSi)_3OH$] species of the silica framework, and the peak at −79.4 ppm corresponds to T^3 [$RSi(OSi)_3$] species. The presence of T^3 species indicates that PTES has been condensed into the silica framework, and the Si–C bonds between phenyl groups and silicon atoms are very stable during the hydrothermal treatment and calcination procedure. With increasing amount of PTES from 5.0% to 10%, the intensities of T^3 peaks increase, suggesting that more organosilane has been incorporated into the silica framework. In the ^{13}C CP/MAS NMR spectrum pattern of as-synthesized $I_{100}(0.10)_a$ (Fig. 6B), the resonance peaks at 127 ppm, 134 ppm, 16.0 ppm, 70.8 ppm, 73.6 ppm, 75.8 ppm are observed. Among them, the peaks at 127 ppm and 134 ppm correspond to the C atoms in phenyl groups, and the others are assigned to the C atoms of the template [14]. After mild (250 °C) calcination, the resonances of the template dramatically decrease, and only faint signals between 60 ppm and 80 ppm could be observed, which should be assigned to the C atoms in the incompletely decomposed template. Meanwhile, the characteristic peaks of C atoms in phenyl groups are preserved, in accordance with the results obtained from the ^{29}Si MAS NMR analysis. These results can be confirmed by the TG analysis.

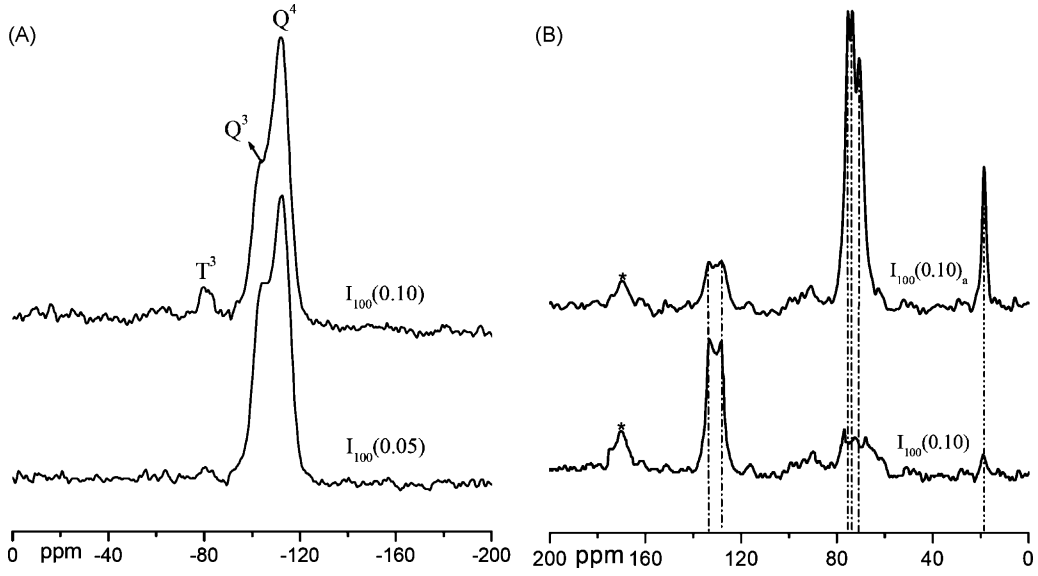

Fig. 6. (A) ^{29}Si MAS NMR spectra of mildly calcined (250 °C) $I_{100}(0.05)$ and $I_{100}(0.10)$; (B) ^{13}C CP/MAS NMR spectra of as-synthesized $I_{100}(0.10)_a$ and mildly calcined (250 °C) $I_{100}(0.10)$. Asterisks denote the spinning sidebands of phenyl groups.

The TG analysis of as-synthesized $I_{100}(0.05, 15)_a$ and $I_{100}(0.10, 15)_a$ materials (Fig. 7A) shows that the weight losses (above 100 °C) concentrate at 182.0 °C and above 300 °C. The former should be due to the decomposition of the template copolymer [5,6], and the latter must include the decomposition of phenyl groups. After mild calcination at 250 °C, the TG-DTG curves of $I_{100}(0.05)$ and $I_{100}(0.10)$ (Fig. 7B) show that the weight loss at 182.0 °C is absent, and only the broad peak above 300 °C (centered at 385.2 °C and 604.9 °C) is observed. Based on the ^{13}C CP/MAS NMR (Fig. 6B), the weight loss at 385.2 °C might be due to the combustion of the residues produced by the incomplete decomposition of the template, and the one at 604.9 °C should be assigned to the decomposition of phenyl groups. With increasing amount of PTES, the weight loss of phenyl groups increases, suggesting that more PTES was incorporated into the silica framework. This result is in accordance with the ^{29}Si MAS NMR analysis (Fig. 6A). The weight loss below 100 °C in the TG-DTG analysis (Fig. 7B) should be attributed to the desorption of the physically adsorbed water. With increasing amount of PTES incorporated, much less amount of water is desorbed, indicating that the pore surface becomes more hydrophobic.

3.2. Modification of Ia-3d mesoporous silicas and their catalytic applications

3.2.1. Preparation of Ia-3d mesoporous phenyl-sulfonic acid catalysts and their applications in the synthesis of Bisphenol A

Bisphenol A is a very important raw material for the production of epoxy resins and other polymers. It is usually obtained by the condensation reaction of phenol with acetone

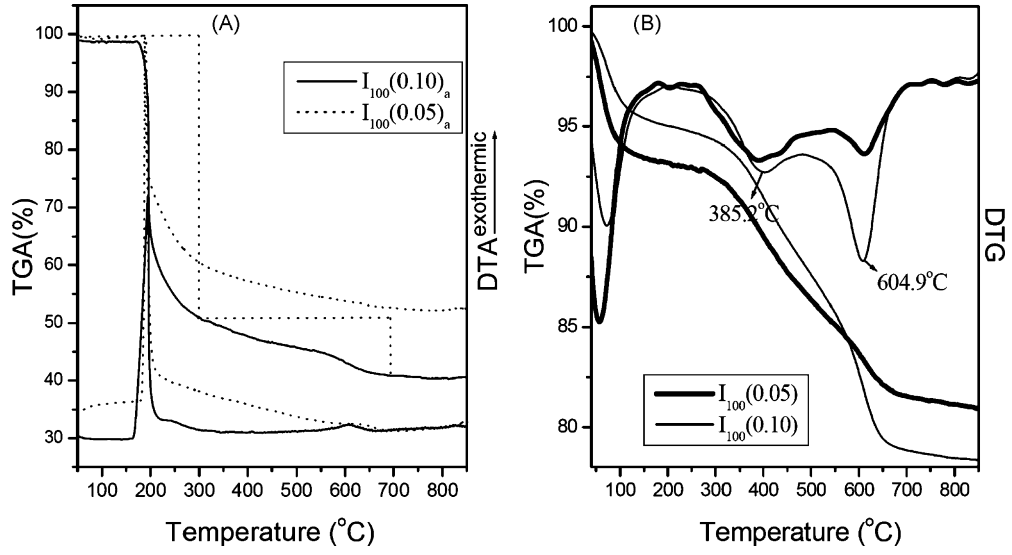

Fig. 7. (A) TG-DTA curves of as-synthesized $I_{100}(0.05)_a$ and $I_{100}(0.10)_a$; (B) TG-DTG curves of mildly calcined (250 °C) $I_{100}(0.05)$ and $I_{100}(0.10)$.

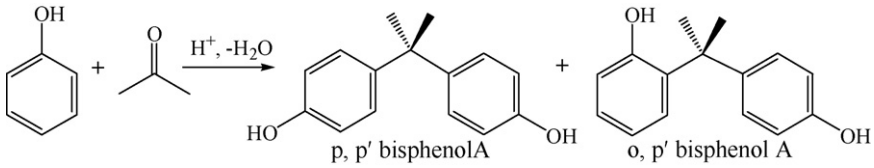

Scheme 1.

in the presence of acid catalysts (Scheme 1), such as heteropolyacid ($H_3PW_{12}O_{40}$) supported on K-10 clay [20], zeolites [21], mesoporous sulfonic acid [22], and ion-exchange resins like Amberlysts. Here we have investigated the catalytic performance of large-pore Ia-3d and 2d-hexagonal mesoporous phenyl-sulfonic acid catalysts in this reaction. For comparison, *p*-toluenesulfonic acid and SBA-15 silica were also used as catalysts. Mesoporous phenyl-sulfonic acid catalysts were prepared by the sulfonation of Ia-3d and 2d-hexagonal materials containing 10% PTES with 25% fuming sulfuric acid in the presence of CH_2Cl_2. Both Ia-3d and 2d-hexagonal sulfonated materials keep the ordered structures of their parent materials, which could be confirmed by the power XRD and N_2 adsorption–desorption measurements (not shown). The introduction of sulfonic acid sites into the channels can be confirmed by the S elemental analysis and the acid–base titration (Table 2).

The "per acid site yield" of all the acid catalysts is listed in Table 2. Under the identical conditions, only *p*,*p*′-Bisphenol A and its isomer *o*,*p*′-Bisphenol A are produced, and other products like trisphenols are not observed while no products are obtained over SBA-15 silica. Among all the catalysts, *p*-toluenesulfonic acid is the most active, probably due to that the acid sites in the homogeneous system could be more easily contacted by reaction reagents than those in the heterogeneous system. In addition, both Ia-3d $I_{100}(0.10)$–SO_3H and 2d-hexagonal $H_{100}(0.10)$–SO_3H mesoporous solid acid catalysts display high catalytic performance. Usually, in the liquid-phase reactions catalyzed by solid catalysts, the larger pore dimension of these solid catalysts is more beneficial to the diffusion of reactants and products, and thus lead to the improvement of their catalytic performance. Surprisingly, though the pore size (5.6 nm) of $H_{100}(0.10)$–SO_3H is larger than that (5.0 nm) of $I_{100}(0.10)$–SO_3H, the catalytic activity of the latter is slightly higher than that of the former (33 versus 30) (Table 2). This inconsistent result should be attributed to that Ia-3d $I_{100}(0.10)$–SO_3H possesses the three-dimensional interwoven channels and the larger surface area. Compared with homogeneous *p*-toluenesulfonic acid, mesoporous solid acid catalysts show higher selectivity to *p*,*p*′-Bisphenol A (Table 2). The selectivity to *p*,*p*′-Bisphenol A (*p*,*p*′/*o*,*p*′ ratio) over $H_{100}(0.10)$–SO_3H is 3.7, slightly higher than that (3.1) over $I_{100}(0.10)$–SO_3H. This phenomenon might be ascribed to that the channels of the Ia-3d catalyst are not straight and not as narrow-ranged as those of the 2d-hexagonal catalyst.

3.2.2. Preparation of amino-functionalized Ia-3d mesoporous base catalysts and their applications in the synthesis of flavanone

Flavanone is an important polyphenolic compound, and widely used to manufacture various medicines. Commonly, flavanone is prepared via the Claisen-Schmidt condensation reaction of benzaldehyde with 2′-hydroxyacetopheone and the subsequent intramolecular Michael reaction of 2′-hydroxychalcone under acidic or basic conditions [23]. Until now some solid catalysts such as barium hydroxides [24], hydrotalcites [25], and natural phosphates modified with $NaNO_3$ or KF [26], have been used for the synthesis of flavanone. Amino-functionalized SBA-15 mesoporous solid base catalysts have also been applied to the preparation of flavanone [27]. Here we have investigated the catalytic activity of large-pore amino-functionalized Ia-3d mesoporous base catalysts ($I_x(y)$-APS) in the synthesis reaction of flavanone. Additionally, we also investigated the effect of pore sizes of $I_x(y)$-APS on their catalytic performance.

As shown in Table 3, the BET surface area, pore size, and pore volume of $I_x(y)$-APS ($x = 35\,^{\circ}C$, $80\,^{\circ}C$ and $100\,^{\circ}C$, respectively) correspondingly decrease in comparison to those of parent materials, which indicates that during the grafting procedure amino groups have been introduced into the channels. This analysis could be confirmed by the presence of the N element in the $I_x(y)$-APS materials (Table 3).

Table 2
Condensation reaction of phenol with acetone to Bisphenol A over different acid catalysts[a]

Catalyst	*S* content (mmol/g final solid)	Acid amount (mmol H^+/g solid)	Bisphenol A (mol)/acid site (mol)	*p*,*p*′/*o*,*p*′ molar ratio
p-TsOH[b]			56	2.0
SBA-15 silica		0.11	–	–
$I_{100}(0.10)$–SO_3H[c]	0.20	0.33 (5.0 nm)[d]	33	3.1
$H_{100}(0.10)$–SO_3H[e]	0.18	0.30 (5.6 nm)[d]	30	3.7

[a] Reaction conditions: 0.10 g catalyst, 60 mmol phenol, 10 mmol acetone, $T = 85\,^{\circ}C$, $t = 24$ h.
[b] *p*-Toluenesulfonic acid.
[c] PTES is prehydrolyzed prior to TEOS in template solution for 15 min.
[d] Pore size (calculated from the adsorption branches).
[e] TEOS is prehydrolyzed prior to PTES in template solution for 60 min.

Table 3
The pore parameters of $I_x(y)$-APS and their catalytic performance in the synthesis of flavanone[a]

Sample	S_{BET} ($m^2\ g^{-1}$)	Pore size (nm)	V_t ($cm^3\ g^{-1}$)	N/Si	Conv. of B (%)	Select. to C (%)	Select. to D (%)	Select. to E (%)
$I_{35}(0.05)$[b]	795	3.8	0.48					
$I_{35}(0.05)$-APS	392	2.9	0.33	6.0	9.2	35.5	64.5	–
$I_{80}(0.05)$[b]	1010	5.6	1.09					
$I_{80}(0.05)$-APS	560	4.9	0.75	6.2	72.4	25.5	56.3	18.2
$I_{100}(0.05)$[b]	1091	6.8	1.25					
$I_{100}(0.05)$-APS	586	6.1	0.79	6.6	84.2	25.0	54.3	20.7

[a] Reaction conditions: 0.20 g catalyst, 10 mmol benzaldehyde, 10 mmol 2′-hydroxyacetonphenone, $T = 140\ ^\circ C$, $t = 15$ h.
[b] Samples were calcined at 550 °C in air for 6 h to remove the template and phenyl groups.

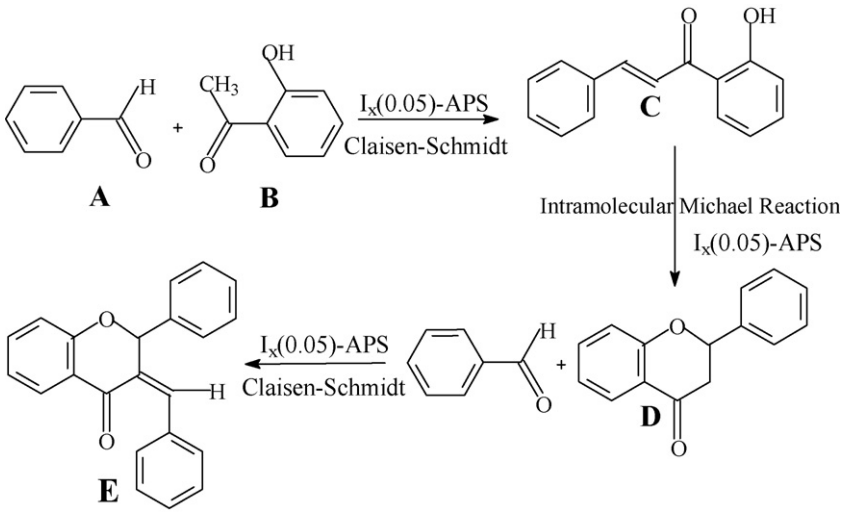

Scheme 2.

According to the analytic results from GC–MS, the products are 2′-hydroxychalcone (C), flavanone (D) and a by product (MW = 312.3) (E), which should be produced by the further Claisen-Schmidt condensation reaction of flavanone with benzaldehyde in the presence of $I_x(y)$-APS base catalysts (Scheme 2). The product E has not been produced when other basic catalysts are used, and the related reaction mechanism is under investigation. The conversion of B and the selectivities to products are shown in Table 3. Under the same reaction conditions, $I_{35}(0.05)$-APS, $I_{85}(0.05)$-APS and $I_{100}(0.05)$-APS, whose pore size are 2.9 nm, 4.9 nm and 6.1 nm, respectively, display distinct catalytic performance. The conversion of B over $I_{35}(0.05)$-APS is only 9.2%. However, those over $I_{85}(0.05)$-APS and $I_{100}(0.05)$-APS are 72.4% and 84.2%, respectively. Since these three mesoporous base catalysts possess the cubic Ia-3d structure, the difference in the conversions of B should be ascribed to their different pore sizes. Therefore, it is believed that in this liquid condensation reaction, the larger pore size of $I_x(y)$-APS base catalysts is more beneficial to the effective diffusion of reactants and products, and thus leads to the increase of the conversion of B. In addition, the pore size of $I_x(0.05)$-APS has a great effect on the distribution of products (Table 3). For $I_{35}(0.05)$-APS, the products are only C and D, and the bulkier E is not observed, which indicate that the small pore size (2.9 nm) of $I_{35}(0.05)$-APS limits the formation of the product E. However, for $I_{85}(0.05)$-APS and $I_{100}(0.05)$-APS, their larger pore size lead to the formation of the product E, and the selectivities to the product E are 18.2% and 19.7%, respectively. With the increase in the pore size of $I_x(0.05)$-APS from 2.9 nm to 6.1 nm, the selectivity to the product C gradually decreases, and the selectivity to products (D + E) correspondingly increases. The selectivities to products (D + E) over $I_{35}(0.05)$-APS, $I_{85}(0.05)$-APS and $I_{100}(0.05)$-APS are 64.5%, 74.5% and 75.0%. These data indicate that the enlargement of the pore size of $I_x(0.05)$-APS is favorable to the intramolecular Michael reaction of 2′-hydroxychalcone (C) to flavanone (D), and thus the further Claisen-Schmidt condensation reaction of flavanone (D) with benzaldehyde to the product E.

4. Conclusions

Templated by triblock copolymer ($EO_{20}PO_{70}EO_{20}$), large pore phenyl-functionalized Ia-3d mesoporous silicas have been synthesized by co-condensation of TEOS and PTES. By the prehydrolysis of PTES prior to TEOS, the ordered Ia-3d materials have been obtained in the PTES molar percentage range of 3.0–10%. By the prehydrolysis of TEOS prior to PTES, the ordered 2d-hexagonal material has also been synthesized. By further modifications, phenyl-sulfonic acid functionalized Ia-3d and 2d-hexagonal mesoporous acid catalysts and amino-functionalized Ia-3d mesoporous base catalysts were successfully prepared. In the condensation reaction of phenol

with acetone to Bisphenol A, both Ia-3d and 2d-hexagonal mesoporous phenyl-sulfonic acid catalysts exhibited high catalytic performance. Due to the three-dimensional channels, the Ia-3d acid catalyst displayed slightly higher catalytic activity than the 2d-hexagonal one. In the synthesis of flavanone, the pore sizes of amino-functionalized Ia-3d mesoporous base catalysts displayed a great effect on their catalytic performance. It was found that with the increase in the pore size of I_x(0.05)-APS, their catalytic performance pronouncedly increased.

Acknowledgements

We thank the National Basic Research Program of China (2004CB217804), the National Natural Science Foundation of China (20673046) and Jilin Province (20020806) for the financial support of this work.

References

[1] C.T. Kresge, M.E. Leonowicz, W.J. Roth, J.C. Vartuli, J.S. Beck, Nature 359 (1992) 710.
[2] A. Corma, Top. Catal. 4 (1997) 249.
[3] P.J. Branton, P.G. Hull, K.S.W. King, J. Chem. Soc., Chem. Commun. (1993) 1257.
[4] D.E. De Vos, M. Dams, B.F. Sels, P.A. Jacobs, Chem. Rev. 102 (2002) 3615.
[5] D. Zhao, J. Feng, Q. Huo, N. Melosh, G.H. Fredrickson, B.F. Chmelka, G.D. Stucky, Science 279 (1998) 548.
[6] D. Zhao, Q. Huo, J. Feng, B.F. Chmelka, G.D. Stucky, J. Am. Chem. Soc. 120 (1998) 6024.
[7] C.A.S. Maria, X.S. Zhao, A.T. Kustedjo, S.Z. Qiao, Micropor. Mesopor. Mater. 72 (2004) 33.
[8] D. Margolese, J.A. Melero, S.C. Christiansen, B.F. Chmelka, G.D. Stucky, Chem. Mater. 12 (2000) 2448.
[9] T. Kang, Y. Park, K. Choi, J.S. Lee, J. Yi, J. Mater. Chem. 14 (2004) 1043.
[10] X. Wang, K.S.K. Lin, J.C.C. Chan, S. Cheng, Chem. Commun. (2004) 2762.
[11] Y. Wang, B. Zibrowius, C. Yang, B. Spliethoff, F. Schüth, Chem. Commun. (2004) 46.
[12] X. Liu, B. Tian, C. Yu, F. Gao, S. Xie, B. Tu, R. Che, L. Peng, D. Zhao, Angew. Chem. Int. Ed. 41 (2002) 3876.
[13] S. Che, A.E. Garcia-Bennett, X. Liu, R.P. Hodgkins, P.A. Wright, D. Zhao, O. Terasaki, T. Tatsumi, Angew. Chem. Int. Ed. 42 (2003) 3930.
[14] Y. Wang, C. Yang, B. Zibrowius, B. Spliethoff, M. Linden, F. Schüth, Chem. Mater. 15 (2003) 5029.
[15] F. Kleitz, S.H. Choi, R. Ryoo, Chem. Commun. (2003) 2136.
[16] J. Tang, C. Yu, X. Zhou, X. Yan, D. Zhao, Chem. Commun. (2004) 2240.
[17] D. Chen, Z. Li, C. Yu, Y. Shi, Z. Zhang, B. Tu, D. Zhao, Chem. Mater. 17 (2005) 3228.
[18] J. Huang, T. Wu, S. Wu, H. Wang, L. Xing, K. Song, H. Xu, Y. Jiang, Q. Kan, Mater. Chem. Phys. 94 (2005) 173.
[19] B. Rác, P. Hegyes, P. Forgo, Á. Molnár, Appl. Catal. A 299 (2006) 193.
[20] G.D. Yadav, N. Kirthivasan, Appl. Catal. 154 (1997) 29.
[21] A.P. Singh, Catal. Lett. 27 (1992) 431.
[22] D. Das, J.-F. Lee, S. Cheng, J. Catal. 223 (2004) 152.
[23] J.B. Harbone, T.J. Mabry, The Flavonoids: Advances in Research, Chapman & Hall, New York, 1982.
[24] A. Fuentes, J.M. Marinas, J.V. Sinisterra, Tetrahedron Lett. 28 (1987) 4541.
[25] M.J. Climent, A. Corma, S. Iborra, A. Velty, J. Catal. 221 (2004) 474.
[26] D.J. Macquarrie, R. Nazih, S. Sebti, Green Chem. 4 (2002) 56.
[27] X. Wang, K.S.K. Lin, J.C.C. Chan, S. Cheng, J. Phys. Chem. B 109 (2005) 1763.